

Original article:

BIOLOGICAL AND QUANTITATIVE-SAR EVALUATIONS, AND DOCKING STUDIES OF (*E*)-*N*-BENZYLIDENEBENZOHYDRAZIDE ANALOGUES AS POTENTIAL ANTIBACTERIAL AGENTS

Mohammad Sayed Alam^{1,2}, Sefat Jebin², M. Mostafizur Rahman², Md. Latiful Bari³, Dong-Ung Lee^{1,*}

¹ Division of Bioscience, Dongguk University, Gyeongju 780-714, Republic of Korea

² Department of Chemistry, Jagannath University, Dhaka 1100, Bangladesh

³ Food analysis and Research laboratory, Centre for Advance Research in Sciences, University of Dhaka, Dhaka-1000, Bangladesh

* Corresponding author: Dong-Ung Lee, Division of Bioscience, Dongguk University, Korea; Tel: +82 54 770 2224; Fax: +82 54 742 9833; E-mail: dulee@dongguk.ac.kr

<http://dx.doi.org/10.17179/excli2016-388>

This is an Open Access article distributed under the terms of the Creative Commons Attribution License (<http://creativecommons.org/licenses/by/4.0/>).

ABSTRACT

A series of 15 (*E*)-*N*-benzylidenebenzohydrazide analogues were evaluated for their antimicrobial activities against eleven pathogenic and food-borne microbes, namely, *S. aureus* (G⁺), *L. monocytogenes* (G⁺), *B. subtilis* (G⁺), *K. pneumonia* (G⁻), *C. sakazakii* (G⁻), *C. freundii* (G⁻), *S. enterica* (G⁻), *S. enteritidis* (G⁻), *E. coli* (G⁻), *Y. pestis* (G⁻), and *P. aeruginosa* (G⁻). Most of the compounds exhibited selective activity against some Gram-negative bacterial strains. Of the compounds tested (**3a-o**), **3b** and **3g** were most active against *C. freundii* (MIC = ~19 µg mL⁻¹). Whereas, compounds **3d**, **3i**, **3k** and **3n** exhibited MIC values ranging from 37.5 to 75 µg mL⁻¹ against *C. freundii*, and compounds **3e**, **3l** and **3n** had MIC values of ~75 µg mL⁻¹ against *K. pneumonia*. Quantitative structure-antibacterial activity relationships were studied using physicochemical parameters and a good correlation was found between calculated octanol-water partition coefficients (clogP; a lipophilic parameter) and antibacterial activities. *In silico* screening was also performed by docking high (**3b** and **3g**) and low (**3n**) activity compounds on the active site of *E. coli* FabH receptor, which is an important therapeutic target. The findings of these *in silico* screening studies provide a theoretical basis for the design and synthesis of novel benzylidenebenzohydrazide analogues that inhibit bacterial FabH.

Keywords: Hydrazone Schiff base, antimicrobial activity, physicochemical properties, docking study

INTRODUCTION

Isoniazid (isonicotinylhydrazide; INH) (Figure 1A) is a front-line antimycobacterial that is usually used to treat tuberculosis. INH exerts its activity *via* a bacterial catalase-peroxidase (KatG) (Suarez et al., 2009) by forming isonicotinic acyl-NADH complex, which interacts firmly to enoyl-acyl carrier protein reductase (InhA), and thus, inhibits the synthesis of mycolic acid, and mycobac-

terial cell growth. A hydrazone Schiff base analogue of INH (Figure 1A) has been reported to have antimycobacterial activity against INH resistant *M. tuberculosis* strains and to exhibit lower toxicity than INH (Sah and Peoples, 1954; Bavin et al., 1954) and nifuroxazide – a commercial hydrazide-hydrazone Schiff base antibiotic used to treat colitis and diarrhea. Another analogue of nifuroxazide was found to show antimicrobial activity comparable to that of ceftriaxone

(Rollas et al., 2002). Currently, bacterial resistance to existing drugs, such as, β -lactam antibiotics, macrolides, quinolones, and vancomycin, is considered one of the most important health concerns (Cassell and Mekalanos, 2001), and thus, sustained research efforts are being made to identify new drugs with wide therapeutic windows, broad spectrum activities, and novel modes of action. A literature survey revealed that synthetics and natural products containing the hydrazone Schiff base or Schiff base motif exert their antibiotic activities by inhibiting fatty acid biosynthesis (FAB) (Cheng et al., 2009; Shi et al., 2010; Song et al., 2014a). In prokaryotic organisms, FAB is crucially required for cell viability and growth (Song et al., 2014b). β -Ketoacyl-acyl carrier protein (ACP) synthase III (FabH or KAS III) plays an important role in bacterial FAB (Khandekar et al., 2003) and is considered an essential functional enzyme in the bacterial FAB system. Bacterial FabH has no homolog in man, and thus, is an attractive target for the design of new antibiotics (Lee et al., 2009 and 2012). The structures of several reported antibacterial FabH inhibitors that possess a Schiff base or hydrazone Schiff base motif are shown in Figure 1B, and interest-

ingly, these structural motifs are also found in many bioactive compounds.

Hydrazone Schiff bases possess -CONHN=CH- moiety and they are widely exploited to syntheses of various biologically active molecules. In addition, they have shown wide-ranging bioactivities. For example, antimicrobial (Vijesh et al., 2013), anti-cancer (Dandawate et al., 2012), anti-mycobacterial (Mahajan et al., 2011), anti-convulsant (Kulandasamy et al., 2009), anti-inflammatory (Rajitha et al., 2011), analgesic (Kümmerle et al., 2009), anti-hypertensive (Leal et al., 2012), anti-platelet (Mashayekhi et al., 2013), and anti-protozoal activities (Carvalho et al., 2012). Hydrazones are also used as herbicides, insecticides, nematocides, rodenticides, plant growth regulators, and housefly sterilants (Akelah et al., 1993; Mohan et al., 1988). Hydrazone Schiff bases are versatile polydentate chelating agents and form a variety of complexes with various transition and inner transition metals with different bioactivities and practical applications (Gad et al., 2000; Zhong et al., 2007; Fan et al., 2010; Juliano et al., 2010). These wide-ranging biochemical activities and uses of hydrazone Schiff bases and their complexes have attracted considerable research attention.

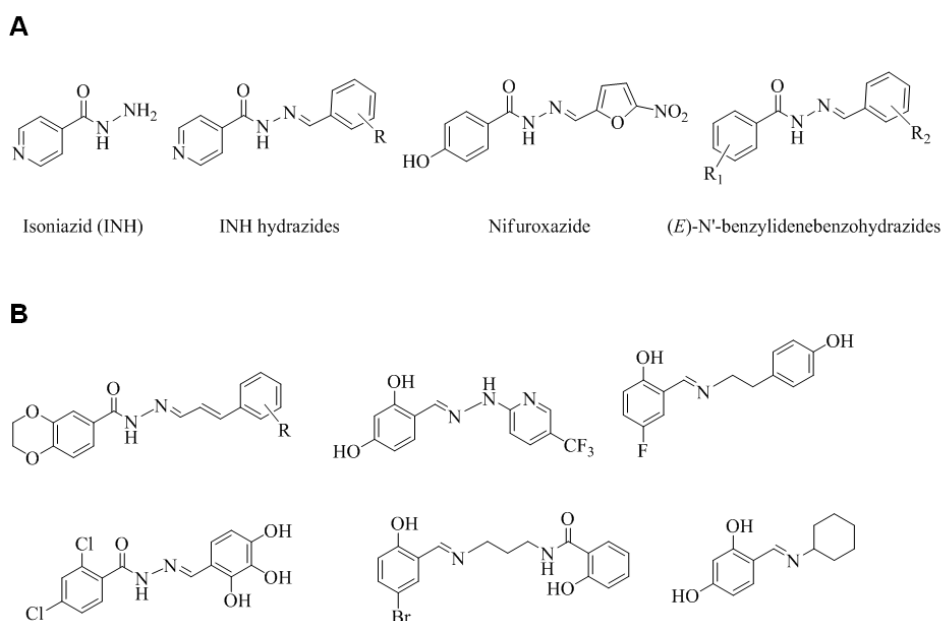


Figure 1: Structures of (A) key molecules and (B) some reported potential FabH inhibitors possessing a hydrazone Schiff base or Schiff base motif

During our continued studies (Alam et al., 2013, 2014, 2015) on novel bioactive compounds, we evaluated the antimicrobial activities of a series of (*E*)-*N'*-benzylidenebenzohydrazide analogues (**3a-o**) exhibiting structural similarities with INH and nifuroxazide. In a previous study, we described the synthesis and cytotoxic and antioxidant activities of a series of fifteen (*E*)-*N'*-benzylidenebenzohydrazide analogues (Alam and Lee, 2016). Here, we report the *in vitro* antibacterial activities of these fifteen (*E*)-*N'*-benzylidenebenzohydrazide analogues (**3a-o**) against 11 pathogenic and food-borne bacterial strains, that is, three Gram-positive (*Staphylococcus aureus*, *Listeria monocytogenes*, and *Bacillus subtilis*), and eight Gram-negative bacterial strains (*Klebsiella pneumoniae*, *Cronobacter sakazakii*, *Citrobacter freundii*, *Salmonella enterica*, *Salmonella enteritidis*, *E. coli*, *Yersinia pestis*, and *Pseudomonas aeruginosa*). In addition, physicochemical characteristics of the synthesized compounds were used to access quantitative structure-antibacterial activity relationships (Q-SAR). Finally, *in silico* screening was performed using docking simulations using the X-ray crystallography determined structure of *E. coli* FabH to investigate the binding affinities and interaction modes of benzylidene-hydrazone analogues at its active site. Computer-assisted drug design (CADD) was used as a useful tool for conducting docking simulations, and provides important information regarding the natures of interactions, favorable bioactive

conformations, and binding affinities of ligands at active sites of target receptors (Alam and Lee, 2016). For these reasons, this technique is helpful for identifying therapeutic lead compounds (Shoichet et al., 2002).

MATERIAL AND METHODS

Chemistry

The (*E*)-*N'*-Benzylidenebenzohydrazide analogues (**3a-o**) examined in the present study were prepared as we previously described (Alam and Lee, 2016) from their corresponding benzohydrazides (**2**) as presented in Figure 2. The mixture of methyl esters of benzoic acid (13.6 g, 0.1 M) or salicylic acid (15.2 g, 0.1 M) and hydrazine hydrate (12.5 g, 0.25 M) in 100 mL ethanol (roughly) were refluxed for 3 h. TLC method was used to observe the reaction progress. The obtained solid products were separated and purified by recrystallization using aqueous ethanol. The structures of the synthesized compounds were characterized by comparing the previously reported physical and spectral data. The benzohydrazides (**2**, 1 mM) so obtained were then refluxed with suitably substituted benzaldehydes (1 mM) in ethanol for 1.5-2.5 h. The reaction progress was monitored by TLC. At room temperature, the reaction mixtures give solid crude products, and they were filtered and crystallized using ethanol to afford the pure compounds (**3a-o**) (81-96 % yield).

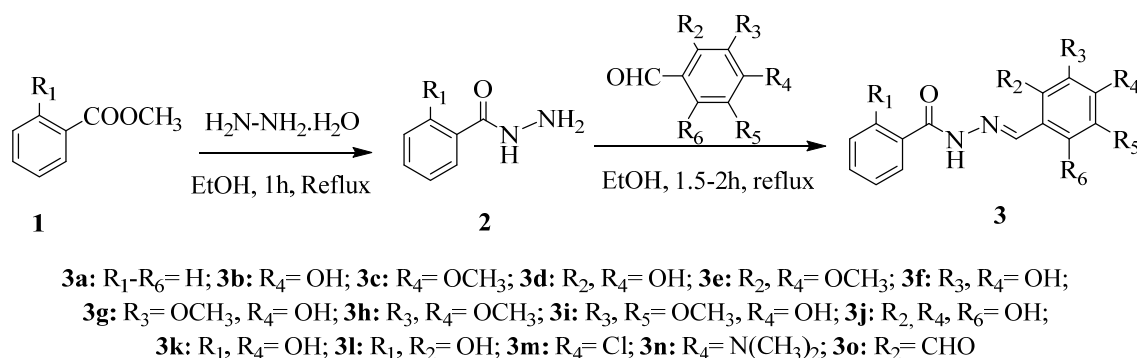


Figure 2: The synthesis of novel (*E*)-*N'*-benzylidenebenzohydrazide analogues **3a-o**

Antibacterial screening

A previously reported filter paper disc diffusion method (Alam and Lee, 2010) was used to determine the *in vitro* antibacterial effects of **3a-o** against eleven bacterial strains. Nutrient agar (NA) media (Difco Laboratories, Lawrence, KS), a bacterial growing medium was inoculated with liquid cultures (0.2 mL) of the microorganisms. Discs soaked with test samples (**3a-o**) were kept on pre-treated agar Petri dishes and incubated aerobically at 37 °C (24 h). DMSO and nalidixic acid were used as negative and positive controls, respectively. Bactericidal activity was defined as inhibitory zones diameters in mm. Evaluations were performed in triplicate.

Minimal inhibitory concentrations (MIC, in µg/mL) against *Klebsiella pneumonia* (JCM 1662) and *Citrobacter freundii* (JCM 1657) were determined using the serial dilution technique (Alam and Lee, 2010) using nutrient broth medium (DIFCO). MIC was

defined as the lowest concentration of the tested compound (in DMSO) that inhibited bacterial growth.

Computational analysis

The molecular geometries of the (*E*)-*N'*-benzylidenebenzohydrazide analogues (**3a-o**) were examined using standard bond length and angles using the ChemBio3D ultra Ver. 14 molecular modeling program (CambridgeSoft Corporation, Cambridge, MA 02140, USA). Physicochemical properties were calculated using Molinspiration Cheminformatics Software (Molinspiration Cheminformatics, SK 90026 Slovensky Grob, SR). The method used for calculating clogP values was developed by Molinspiration (miLogP2.2-2005) derived from the group contributions of more than twelve thousand drug-like compounds, and the theoretical logP and experimental logP values were used as a training set for fitting correc-

Table 1: *In vitro* antimicrobial profiles of (*E*)-*N'*-benzylidenebenzohydrazide analogues (**3a-o**) as determined by growth inhibition zones

Comp.	Gram-positive			Gram-negative							
	S. a.	L. m.	B. s.	K. p.	C. s.	C. f.	S. e.	S. t.	E. c.	Y. p.	P. a.
3a	-	-	-	-	-	-	-	-	-	-	-
3b	-	-	-	13±0.5	-	30±1.5	-	-	14±0.5	-	-
3c	-	-	-	-	-	-	-	-	-	-	-
3d	-	-	-	14±0.5	14±0.5	25±1.0	-	-	14±0.5	-	-
3e	11±1.0	10±1.0	10±1.0	17±1.0	8±0.5	10±1.0	-	10±1.0	8±1.0	10±0.5	12±1.0
3f	-	-	-	13±0.5	-	-	9±1.0	-	15±0.5	-	-
3g	-	-	-	13±0.5	-	30±1.0	-	-	13±0.5	-	11±1.0
3h	-	-	-	-	-	-	-	-	-	-	-
3i	-	-	-	-	-	23±0.5	12±1.0	-	15±1.0	-	-
3j	-	-	-	-	-	-	8±1.0	-	-	-	-
3k	-	-	-	14±0.5	-	22±0.5	-	-	11±1.0	-	-
3l	7±0.5	-	-	17±0.5	-	9±0.5	7±0.5	-	8±0.5	-	-
3m	-	-	-	-	-	-	-	-	-	-	-
3n	-	-	-	16±0.5	-	19±1.5	-	-	12±0.5	-	-
3o	-	-	-	-	-	-	-	-	-	-	-
NA	24±1.0	8.0±0.5	20±1.0	21±1.0	24±1.0	29±1.5	10±1.0	18±1.0	24±1.0	-	23±1.0

Inhibitory activities are expressed as diameters (in mm) of observed inhibitory zones. (-), Not active. The activities presented are the means ± SDs (three experiments). S. a., *Staphylococcus aureus* (JMC 2151); L. m., *Listeria monocytogenes* (ATCC 43256); B. s., *Bacillus subtilis* (IFO 13719); K. p., *Klebsiella pneumoniae* (JCM 1662); C. s., *Cronobacter sakazakii* (CARS 2012-J-F); C. f., *Citrobacter freundii* (JCM 1657); S. e., *Salmonella enterica* (ATCC 10708); S. t., *Salmonella enteritidis* (ATCC 13076); E. c., *E. coli* (CARS 2011-016); Y. p., *Yersinia pestis* (CARS 2013-027); P. a., *Pseudomonas aeruginosa* (PA01)

tion factors. The molecular polar surface area (PSAs) were obtained as sums of fragment contributions (Ertl et al. 2000). Molecular lipophilicity potentials (MLPs) and PSAs maps were analyzed using Molinspiration Galaxy 3D Structure Generator (ver. 2013.02 beta).

Docking studies

The molecular geometries of compounds **3c**, **3i** and **3j** were constructed using standard bond lengths and angles as mentioned above, and energy minimized using the Hartree-Fock method at 6-31G basis set with R-Closed-Shell wave function in the ChemBio3D Ultra Ver. 14.0 software (GAMESS Interface). The docking studies were performed using crystal structure of *E. coli* FabH-CoA complex retrieved from the Protein Data Bank (PDB code: 1HNJ). To prepare the receptor for docking studies, co-crystallized ligand and water molecules were removed, while polar hydrogen atoms and Kollman-united charges were included to the FabH receptor molecule. The necessary pdb and pdbqt files of ligands and *E. coli* FabH receptor were prepared using AutoDock 4.2 software (Morris et al., 2009). The study was carried out using the usual docking protocol applied for AutoDock Vina in PyRx 0.8 software (Trott and Olson, 2010) where free rotation was allowed through single bonds of ligands. The docking results were analyzed using Discovery Studio 4.0 (Accelrys, Inc. San Diego, CA 92121, USA) and binding scores were calculated using iGEMDOCK software (Yang and Chen, 2004).

RESULTS AND DISCUSSION

Antibacterial activities

Compounds **3a-o** were evaluated for their *in vitro* antibacterial activities against three Gram-positive bacteria, *S. aureus*, *L. monocytogenes*, and *B. subtilis*, and eight Gram-negative bacteria *K. pneumonia*, *C. sakazakii*, *C. freundii*, *S. enterica*, *S. enteritidis*, *E. coli*, *Y. pestis*, and *P. aeruginosa* by disc diffusion. As presented in Table 1, compound **3e** inhibited the growths of all

bacterial strains except *S. enterica*, but its activity was relatively weak. A half of the tested compounds inhibited G(-)-bacteria *K. pneumonia*, *C. freundii*, and *E. coli*, but only **3e** inhibited G(+)-bacteria. Of the compounds tested, **3b** and **3g** were most effective against *C. freundii*, and had activities similar to nalidixic acid (the positive standard). Compounds bearing an OH group at the R₄-position (*para*-position) in the benzylidene phenyl ring (e.g., **3b**, **3g** > **3d** > **3i** > **3k**) better inhibited *C. freundii*. Whereas, compounds with additional OH substitution at the *meta*-position (e.g. **3f**) or *ortho*-positions (e.g. **3j**) were devoid of activity.

The minimal inhibitory concentrations (MICs) of selected compounds were determined against *K. pneumonia* and *C. freundii*; results are summarized in Table 2. Compounds **3b** and **3g** had the lowest MIC values (18.75 µg/mL), followed by **3d**, **3i**, and **3k** (37.5 µg/mL) against *C. freundii*, whereas compounds **3e**, **3l**, and **3n** had similar MIC values (75 µg/mL) against *K. pneumonia*. Above results indicate the presence of a polar hydroxyl group at the R₄-position (*para*-position) favors activity, but that *meta* positioned OH groups reduce activity.

Table 2: MIC of some (E)-N'-benzylidenebenzohydrazide analogues derivatives against selected bacterial strains

Comp.	MIC, µg/mL	
	<i>K. pneumonia</i>	<i>C. freundii</i>
3b	-	18.75
3d	-	37.5
3e	75	-
3g	-	18.75
3i	-	37.5
3k	-	37.5
3l	75	-
3n	75	75
NA	12.5	6.25

(-), Not measured; MIC, Minimum inhibitory concentration; NA, Nalidixic acid.

Quantitative-SAR study

To explain quantitative structure-antibacterial activity relationships (Q-SAR) of the fifteen (*E*)-*N'*-benzylidenebenzohydrazide analogues (**3a-o**), physicochemical calculations were conducted using ChemBio3D Pro 12 molecular modeling (CambridgeSoft Corporation, Cambridge, MA 02140, USA) and Molinspiration Cheminformatics software (Molinspiration Cheminformatics, SK 90026 Slovensky Grob, SR). The physicochemical properties of molecules, such as, their lipophilicities and polar surface areas (PSAs) play important roles in determining biological responses, and are commonly used to study the structure-activity relationships of bioactive molecules in medicinal chemistry (Alam et al., 2013; Desai et al., 2014). These parameters are now well-accepted major experimental and theoretical tools for drug design and discovery. The physicochemical parameters of all synthesized compounds are listed in Table 3.

In the present study, a considerable number of compounds were found to be active against *K. pneumonia*, *C. freundii*, and *E. coli*. It is well-known that the octanol-water

partition coefficient (logP) of a molecule depends on its hydrophobicity and polarity, which facilitate transit across cellular membranes. Therefore, we examined the correlation between the inhibitory effects of **3a-o** against *K. pneumonia*, *C. freundii*, and *E. coli* and their clogP values. The correlation coefficients (r^2) between clogP values and the inhibitory potencies of active molecules against *K. pneumonia*, *C. freundii*, and *E. coli* were; 0.86 (n = 8; **3b**, **3d-3g**, **3k**, **3l** and **3n**), 0.75 (n = 8; **3b**, **3d,3e**, **3g**, **3i**, **3k**, **3l**, and **3n**), and 0.71 (n = 9; **3b**, **3d-3g**, **3i**, **3k**, **3l**, and **3n**), respectively. Although only a relatively small number of compounds were examined, significant correlations were observed, whereby antibacterial activity increased with clogP against *K. pneumonia* but decreased with clogP against *C. freundii* and *E. coli* (Figure 3). However, the above correlations should be treated with caution because the clogP values of **3a**, **3c**, **3h**, **3m**, and **3o** fell within the medium range for active compounds, but they were in fact inactive. Therefore, we compared maps of lipophilicity potential (MLP) and PSA of two selected active and inactive compounds (**3b** and **3g**

Table 3: Molinspiration calculations of the molecular properties of (*E*)-*N'*-benzylidenebenzohydrazide analogues (**3a-o**)

Comp.	MW (g/mol)	clogP ^a	TPSA ^b	OH-NH interact ^c	O-N interact ^d	nrotb ^e	volume
3a	224.263	3.099	41.462	1	3	3	210.098
3b	240.262	2.619	61.69	2	4	3	218.116
3c	254.289	3.155	50.696	1	4	4	235.644
3d	256.261	2.536	81.918	3	5	3	226.134
3e	284.315	3.14	59.93	1	5	5	261.19
3f	256.261	2.13	81.918	3	5	3	226.134
3g	270.288	2.438	70.924	2	5	4	243.662
3h	284.315	2.745	59.93	1	5	5	261.19
3i	300.314	2.454	80.158	2	6	5	269.208
3j	272.26	2.452	102.146	4	6	3	234.152
3k	256.261	2.56	81.918	3	5	3	226.134
3l	256.261	3.528	81.918	3	5	3	226.134
3m	258.708	3.777	41.462	1	3	3	223.634
3n	267.332	3.201	44.7	1	4	4	256.004
3o	252.273	2.841	58.533	1	4	4	229.082

^aCalculated octanol/water partition coefficients; ^bMolecular polar surface areas; ^cNumbers of hydrogen-bond donors; ^dNumbers of hydrogen-bond acceptors; ^eNumbers of rotatable bonds

vs. **3a** and **3c**). It was found that lipophilicity potentials and the polar surface areas of these two pairs of compounds differed (Figure 4). These results suggest that the distributions of more hydrophilic and polar areas at the *para*-position of benzylidene phenyl ring importantly determine activity against specific bacterial strains.

Molecular docking studies

β -Ketoacyl-(acyl-carrier-protein) synthase III (FabH), a key bacterial enzyme plays a crucial regulatory role in bacterial fatty acid synthesis (FAS) by initiating fatty acid elongation cycles and providing feedback regarding the regulation of FAS, which is essentially required for prokaryotic cell metabolism, viability, and growth. However, the bacterial FAS pathway differs considerably from in man, and bacterial FabH proteins are highly conserved at the sequence and structural level and show no significant homology with any human protein. In addition, the active site residues of FabH receptor are common for Gram-positive and -negative bacterial strains (Nie et al., 2005). These features make FabH protein a potential therapeutic target for the design of novel and broad-spectrum antimicrobial agents as selective and nontoxic FabH inhibitors. To predict the binding affinities of hydrazone Schiff base analogues to FabH, molecular docking of (*E*)-*N'*-benzylidenebenzohydrazide analogues having high (**3b** and **3g**)

and low (**3n**) activity with the active site of *E. coli* FabH receptor was performed. The crystal structure of *E. coli* FabH-CoA complex (Qiu et al., 2001) was retrieved from the Protein Data Bank (PDB ID: 1HNJ) and compounds **3b**, **3g**, and **3n** were docked at its active site using a standard docking protocol. *In silico* docking results are presented in Table 4.

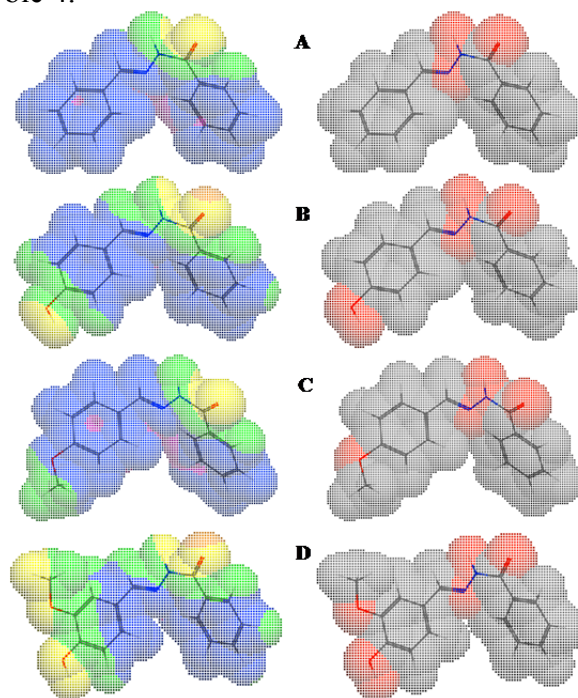


Figure 4: Molecular lipophilicity potentials (left) and polar surface areas (right) of **3a** (A), **3b** (B), **3c** (C), and **3g** (D) showing areas of lipophilicity (blue), intermediate lipophilicity (pink), hydrophilicity (yellow), intermediate hydrophilicity (green), nonpolar (gray/white), and polar (red) areas.

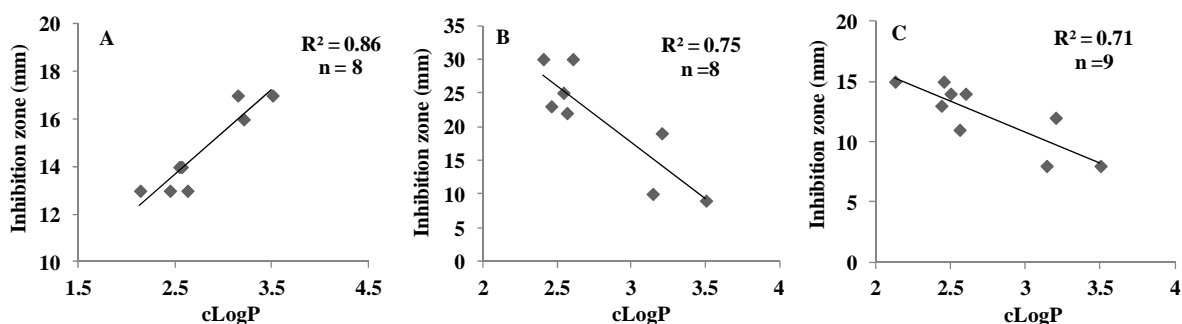


Figure 3: Correlations between inhibition zones (mm) and calculated octanol-water partition coefficients (clogP) of active (*E*)-*N'*-benzylidenebenzohydrazide analogues against (A) *K. pneumonia* (**3b**, **3d-g**, **3k**, **3l** and **3n**), (B) *C. freundii* (**3b**, **3d**, **3e**, **3g**, **3i**, **3k**, **3l** and **3n**), and (C) *E. coli* (**3b**, **3d-g**, **3i**, **3k**, **3l** and **3n**).

Table 4: Docking energies and molecular interactions of the ligand molecules (**3b**, **3g**, and **3n**) with *E. coli* FabH receptor

Entry	Binding affinity (kcal/mol)	Energy contribution		AverConPair	H-bonding residues (distance, Å)	Hydrophobic interactions residues
		vdW	H-bond			
3b	-80.36	-71.29	-9.07	25.72	-	Ala111, Cys112, Leu142, Ile156, Phe157, Leu189, Thr190, Leu191, Leu205, Met207, Val212, Phe213, Ala246, Ile250, Gly305
3g	-84.33	-71.92	-12.41	26.20	Leu189 (2.96)	Leu142, Ile156, Phe157, Leu205, Val212, Phe213, Asn247, Ala246, Ile250, Ser276, Gly305, Gly307
3n	-72.22	-72.22	-	23.70	-	Ala109, Ala110, Leu142, Thr145, Thr190, Leu191, Leu205, Ser276, Thr309

These studies revealed that all three compounds bind to the same active site of FabH receptor as endogenous malonyl-CoA ligand and other reported hydrazone and Schiff base FabH inhibitors (Song et al., 2014a; Zhou et al., 2013; Shi et al., 2010). The binding modes and the different types of interactions found for compound **3b** (most active) and **3n** (least active) were compared and are shown in Figures 5 and 6, respectively. To measure the affinity of ligands for the receptor, we analyzed binding scores for compounds **3b**, **3g**, and **3n** by iGEMDOCK software (Yang and Chen, 2004); results are shown in Table 4. According to docking scores, the high activity compounds **3b** and **3g** had higher binding affinities with FabH receptor than **3n** (the binding energies of **3b**, **3g** and **3n** were -80.36, -84.33, and -72.22 kcal/mol, respectively). Regarding total binding energies, van der Waal contributions for **3b** and **3g** were -71.29 and 71.02 kcal/mol, respectively, and H-bond contributions were -9.07 and 12.41 kcal/mol, respectively. While for **3b** only van der Waal interactions (-72.22 kcal/mol) contributed to total binding energy. In the binding model of **3b** and *E. coli* FabH receptor, two π -sulfur interactions were observed between the benzoyl-phenyl ring and Met207 (3.95 Å) and be-

tween the benzylidene-phenyl ring and Cys112 (4.88 Å), together with π -alkyl interactions with Ala111(4.22 Å), Leu142 (4.81 Å), Leu189 (5.07 Å), Leu191 (5.36 Å), Leu205 (5.19 Å), Val212(5.47 Å), and Ala246 (3.59 Å). However, in the binding model of **3g** with *E. coli* FabH receptor, a H-bond between the carbonyl group of Leu189 (C...H-O: 2.96 Å) and methoxy proton, and π -sulfur and π -sigma interactions of Met207 (3.83 Å) and Ala246 (2.59 Å), respectively were observed including π -alkyl interactions with Ala111 (3.84 Å), Cys112 (5.32 Å), Leu142 (5.07 Å), Leu189 (5.08 Å), and Leu191 (5.48 Å). Whereas in the binding model of **3n** with *E. coli* FabH receptor, no H-bond, π -sulfur, or π -sigma interactions were observed, although π -alkyl interactions with Ala109 (4.65 Å), Ala111 (4.45 Å), Leu189 (4.43 Å), Leu191 (5.34 Å), Leu205 (5.27 Å), and Gly306 (4.43) involving benzoyl- and benzylidene-phenyl rings were observed. In addition, the following van der Waal's interactions were also observed: between **3b** and Cys112, Ile156, Phe157, Thr190, Met207, Phe213, Ile250, and Gly305; between **3g** and Ile156, Phe157, Leu205, Val212, Phe213, Asn247, Ala246, Ile250, Ser276, Gly305, and Gly307; and be-

tween **3n** and Ala110, Leu142, Thr145, Thr190, Ser276, and Thr309. These results indicate compounds **3b**, **3g**, and **3n** bind to the same active site of FabH receptor. However, the most active compounds **3b** (Figure 5) and **3g** (figure not shown) attached more

tightly in the active site of FabH receptor due to additional H-bond, π -sulfur, π -sigma, and hydrophobic interactions, which resulted in higher binding affinities than compound **3n** (Figure 6).

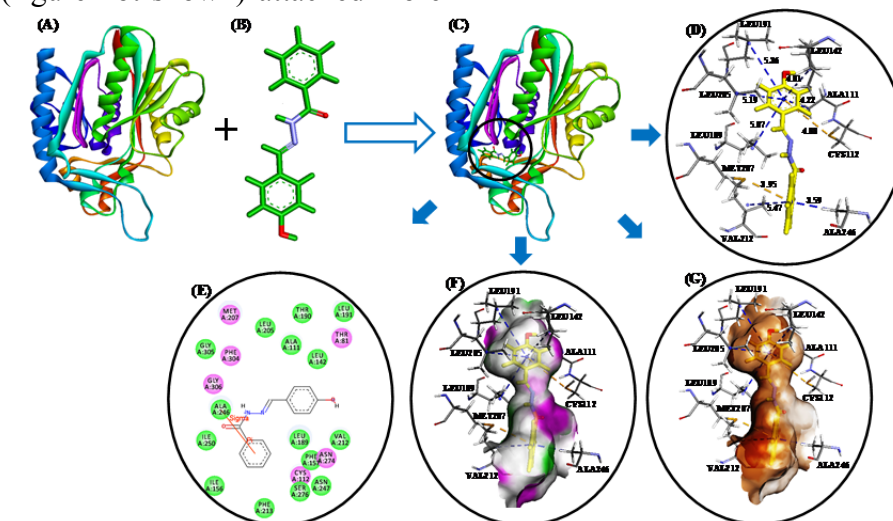


Figure 5: (A) *E. coli* FabH receptor (PDB ID: 1HNJ). (B) HF/6-31G optimized geometry of ligand **3b**. (C) Docked ligand-receptor complex (the circle shows the ligand binding site) (D) Binding model of **3b** with *E. coli* FabH; π -alkyl and π -sulfur interactions are shown by *blue* and *yellow broken lines*, respectively. (E) 2D view of interacting essential amino acid residues at the ligand binding site; The residues involved in electrostatic and covalent interactions are shown by *purple circles* and amino acids involved in van der Waals interactions are shown by *green circles*. (F) Showing hydrogen bond donor (pink) and acceptor (green) surfaces. (G) Showing hydrophobic interactions (brown) surfaces.

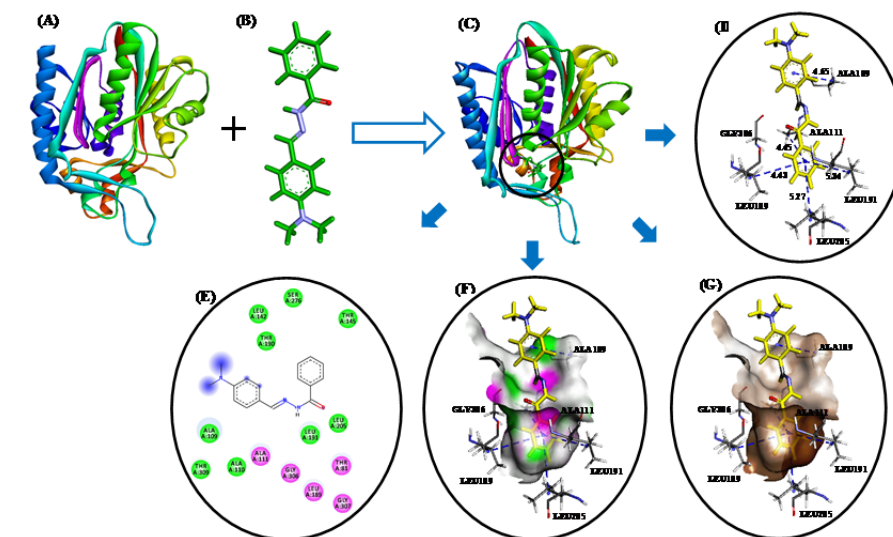


Figure 6: (A) *E. coli* FabH receptor (PDB ID: 1HNJ). (B) HF/6-31G optimized geometry of ligand **3n**. (C) Docked ligand-receptor complex (the circle indicates the ligand binding site) (D) Binding model of compound **3n** with *E. coli* FabH; H-bond and π -alkyl interactions are shown by *red* and *blue broken lines*, respectively. (E) 2D view of interacting essential amino acid residues at the ligand binding site; The residues involved in electrostatic and covalent interactions are shown by *purple circles* and amino acids involved in van der Waals interactions are shown by *green circles*. (F) Showing hydrogen bond donor (pink) and acceptor (green) surfaces. (G) Showing hydrophobic interactions (brown) surfaces.

CONCLUSION

The present study reports the antibacterial activities of a series of 15 (*E*)-*N'*-benzylidenebenzohydrazide analogues against eleven pathogenic and food-borne bacterial strains, of these eleven, three were Gram-positive, i.e., *S. aureus*, *L. monocytogenes*, and *B. subtilis*, and eight were Gram-negative, i.e., *K. pneumoniae*, *C. sakazakii*, *C. freundii*, *S. enterica*, *S. enteritidis*, *E. coli*, *Y. pestis*, and *P. aeruginosa*. The compounds subjected to antibacterial assay, **3b** and **3g**, which are containing one OH group at the *para*-position of the benzylidene phenyl ring, showed lowest MIC values against *C. freundii*. Physicochemical calculations indicated that the antibacterial activities of (*E*)-*N'*-benzylidenebenzohydrazide analogues (**3b**, **3d-3g**, **3i**, **3k**, **3l**, and **3n**) against *K. pneumoniae*, *C. freundii*, and *E. coli* correlated well with calculated logP values. *In silico* screening using molecular docking studies were performed to predict the binding affinities and modes of interaction of the most active (**3b** and **3g**) and least active (**3n**) compounds to the active site of *E. coli* FabH receptor. Compounds **3b** and **3g** were found to bind effectively to the active site of *E. coli* FabH receptor with high affinity, suggesting their potentials as FabH inhibitors. We believe the above findings can be used to facilitate the design and synthesis of novel benzylidenehydrazone analogues as potential antibacterial as FabH inhibitors.

REFERENCES

- Akelah A, Kenawy ER, Sherrington DC. Agricultural polymers with herbicide/fertilizer function-III. Polyureas and poly(Schiff base)s based systems. *Eur Polym J*. 1993;29:1041-5.
- Alam MS, Lee DU. Facile synthesis and antibacterial activity of naturally occurring 5-methoxyfuroflavone. *Chem Pharm Bull*. 2010;58:1643-5.
- Alam MS, Lee DU. Synthesis, biological evaluation, drug-likeness, and *in silico* screening of novel benzylidene-hydrazone analogues as small molecule anticancer agents. *Arch Pharm Res*. 2016;39:191-201.
- Alam MS, Nam YJ, Lee DU. Synthesis and evaluation of (*Z*)-2,3-diphenyl acrylonitrile analogues as anticancer and antimicrobial agent. *Eur J Med Chem*. 2013;69:790-7.
- Alam MS, Lee DU, Bari ML. Antibacterial and cytotoxic activities of Schiff base analogues of 4-aminoantipyrine. *J Korean Soc Appl Biol Chem*. 2014;57:613-9.
- Alam MS, Mostafizur Rahman SM, Lee DU. Synthesis, biological evaluation, quantitative-SAR and docking studies of novel chalcone derivatives as antibacterial and antioxidant agents. *Chem Papers*. 2015;69:1118-29.
- Bavin EM, Drain DJ, Seiler M, Seymour DE. Some further studies on tuberculostatic compounds. *J Pharm Pharmacol*. 1954;4:844-55.
- Carvalho SA, Feitosa LO, Soares M, Costa TE, Henriques MG, Salomão K, et al. Design and synthesis of new (*E*)-cinnamic *N*-acylhydrazones as potent antitrypanosomal agents. *Eur J Med Chem*. 2012;54:512-21.
- Cassell GH, Mekalanos J. Development of antimicrobial agents in the era of new and reemerging infectious diseases and increasing antibiotic resistance. *J Am Med Assoc*. 2001;285:601-5.
- Cheng K, Zheng QZ, Qian Y, Shi L, Zhao J, Zhu HL. Synthesis, antibacterial activities and molecular docking studies of peptide and Schiff bases as targeted antibiotics. *Bioorg Med Chem*. 2009;17:7861-71.
- Dandawate P, Khan E, Padhye S, Gaba H, Sinha S, Deshpande J, et al. Synthesis, characterization, molecular docking and cytotoxic activity of novel plumbagin hydrazones against breast cancer cells. *Bioorg Med Chem Lett*. 2012;22:3104-8.
- Desai NC, Satodiya HM, Kotadiya GM, Vaghani HV. Synthesis and antibacterial and cytotoxic activities of new *N*-3 substituted thiazolidine-2,4-dione derivatives bearing the pyrazole moiety. *Arch Pharm*. 2014;347:23-32.
- Ertl P, Rohde B, Selzer P. Fast calculation of molecular polar surface area (PSA) as a sum of fragment-based contributions and its application to the prediction of drug transport properties. *J Med Chem*. 2000;43:3714-7.
- Fan CD, Su H, Zhao J, Zhao BX, Zhang SL, Miao JY. A novel copper complex of salicylaldehyde pyrazole hydrazone induces apoptosis through up-regulating integrin $\beta 4$ in H322 lung carcinoma cells. *Eur J Med Chem*. 2010;45:1438-46.

- Gad AM, El-Dissouky A, Mansour EM, El-Maghraby A. Thermal stability of poly acryloyl benzoic hydrazide and its complexes with some transition metals. *Polym Degrad Stabil.* 2000;68:153-8.
- Juliano C, Mattana A, Solinas C. Versatile coordinating behaviour of bis(acylhydrazone) ligands derived from imino- and methyl-iminodiacetic acid diethyl ester. Antimicrobial properties of their trinuclear copper(II) complexes. *Transition Met Chem.* 2010;35:253-61.
- Khandekar SS, Daines RA, Lonsdale JT. Bacterial β -ketoacyl-Acyl carrier protein synthases as targets for antibacterial agents. *Curr Protein Pept Sci.* 2003;4:21-9.
- Kümmerle AE, Vieira MM, Schmitt M, Miranda AL, Fraga CA, Bourguignon JJ, et al. Design, synthesis and analgesic properties of novel conformationally-restricted N-acylhydrazones (NAH). *Bioorg Med Chem Lett.* 2009;19:4963-66.
- Kulandasamy R, Adhikari AV, Stables JP. A new class of anticonvulsants possessing 6 Hz activity: 3,4-dialkyloxy thiophene bishydrazones. *Eur J Med Chem.* 2009;44:4376-84.
- Leal CM, Pereira SL, Kümmerle AE, Leal DM, Tesch R, de Sant'Anna CM, et al. Antihypertensive profile of 2-thienyl-3,4-methylenedioxy benzoylhydrazone is mediated by activation of the A2A adenosine receptor. *Eur J Med Chem.* 2012;55:49-57.
- Lee JY, Jeong KW, Lee JU, Kang DI, Kim Y. Novel *E. coli* β -ketoacyl-acyl carrier protein synthase III inhibitors as targeted antibiotics. *Bioorg Med Chem.* 2009;17:1506-13.
- Lee JY, Jeong KW, Shin S, Lee JU, Kim Y. Discovery of novel selective inhibitors of *Staphylococcus aureus* β -ketoacyl acyl carrier protein synthase III. *Eur J Med Chem.* 2012;47:261-9.
- Mahajan A, Kremer L, Louw S, Guérardel Y, Chibale K, Biot C. Synthesis and *in vitro* antitubercular activity of ferrocene-based hydrazones. *Bioorg Med Chem Lett.* 2011;21:2866-8.
- Mashayekhi V, Haj Mohammad Ebrahim Tehrani K, Amidi S, Kobarfard F. Synthesis of novel indole hydrazone derivatives and evaluation of their antiplatelet aggregation activity. *Chem Pharm Bull.* 2013;61:144-50.
- Mohan M, Gupta MP, Chandra L, Jha NK. Synthesis, characterization and antitumour properties of some metal(II) complexes of 2-pyridinecarboxaldehyde 2'-pyridyl hydrazone and related compounds. *Inorg Chim Acta.* 1988;151:61-8.
- Morris GM, Huey R, Lindstrom W, Sanner MF, Bewley RK, Goodsell DS, et al. AutoDock4 and AutoDockTools4: Automated docking with selective receptor flexibility. *J Comput Chem.* 2009;30:2785-91.
- Nie Z, Perretta C, Lu J, Su Y, Margosiak S, Gajiwala KS, et al. Structure-based design, synthesis, and study of potent inhibitors of β -ketoacyl-acyl carrier protein synthase III as potential antimicrobial agents. *J Med Chem.* 2005;48:1596-606.
- Qiu XY, Janson CA, Smith WW, Head M, Lonsdale J, Konstantinidis AK. Refined structures of β -ketoacyl-acyl carrier protein synthase III. *J Mol Biol.* 2001;307:341-56.
- Rajitha G, Saideepa N, Praneetha P. Synthesis and evaluation of N-(α -benzamido-cinnamonyl)-arylhydrazone derivative for anti-inflammatory and antioxidant activities. *Indian J Chem.* 2011;50B:729-33.
- Rollas S, Gulerman N, Erdeniz H. Synthesis and antitubercular activity of some new hydrazones of 4-fluorobenzoic acid hydrazide and 3-acetyl-2,5-disubstituted-1,3,4-oxadiazolines. *IL Farmaco.* 2002;57:171-4.
- Sah PPT, Peoples SA. Isonicotinyl hydrazones as antitubercular agents and derivatives for identification of aldehydes and ketones. *J Am Pharm Assoc.* 1954;43:513-24.
- Shi L, Fang RQ, Zhu ZW, Yang Y, Cheng K, Zhong WQ, et al. Design and synthesis of potent inhibitors of β -ketoacyl-acyl carrier protein synthase III (FabH) as potential antibacterial agents. *Eur J Med Chem.* 2010;45:4358-64.
- Shoichet BK, McGovern SL, Wei B, Irwin JJ. Lead discovery using molecular docking. *Curr Opin Chem Biol.* 2002;6:439-46.
- Song X, Yang Y, Zhao J, Chen Y. Synthesis and antibacterial activity of cinnamaldehyde acylhydrazone with a 1,4-benzodioxan fragment as a novel class of potent β -ketoacyl-acyl carrier protein synthase III (FabH) inhibitor. *Chem Pharm Bull.* 2014a;62:1110-8.
- Song H, Ao GZ, Li HQ. Novel FabH inhibitors: an updated article literature review (July 2012 to June 2013). *Expert Opin Ther Pat.* 2014b;24:19-27.
- Suarez J, Ranguelova K, Jarzecki AA, Manzerova J, Krymov V, Zhao X, et al. An oxyferrous heme/protein-based radical intermediate is catalytically competent in the catalase reaction of *Mycobacterium tuberculosis* catalase-peroxidase (KatG). *J Biol Chem.* 2009;284:7017-29.

Trott O, Olson AJ. AutoDock Vina: Improving the speed and accuracy of docking with a new scoring function, efficient optimization, and multithreading. *J Comput Chem.* 2010;31:455-61.

Vijesh AM, Isloor AM, Shetty P, Sundershan S, Fun HK. New pyrazole derivatives containing 1,2,4-triazoles and benzoxazoles as potent antimicrobial and analgesic agents. *Eur J Med Chem.* 2013;62:410-5.

Yang JM, Chen CC. GEMDOCK: A generic evolutionary method for molecular docking. *Proteins.* 2004; 55:288-304.

Zhong X, Wei HL, Liu WS, Wang DQ, Wang X. The crystal structures of copper(II), manganese(II), and nickel(II) complexes of a (*Z*)-2-hydroxy-*N'*-(2-oxo-indolin-3-ylidene) benzohydrazide-potential anti-tumor agents. *Bioorg Med Chem Lett.* 2007;17:3774-7.

Zhou Y, Du QR, Sun J, Li JR, Fang F, Li DD, et al. Novel Schiff-base-derived FabH inhibitors with diox-ygenated rings as antibiotic agents. *Chem Med Chem.* 2013;8:433-41.